tvst

Article

Topical Corneal Cross-Linking Solution Delivered Via Corneal Reservoir in Dutch-Belted Rabbits

Mariya Zyablitskaya[1], Charles Jayyosi[2], Anna Takaoka[1], Kristin M. Myers[2], Leejee H. Suh[1], Takayuki Nagasaki[1], Stephen L. Trokel[1], and David C. Paik[1]

[1] Department of Ophthalmology, Columbia University, New York, NY, USA
[2] Department of Mechanical Engineering, Columbia University, New York, NY, USA

Correspondence: David C. Paik, MD, Laboratory for Tissue Cross-linking, Department of Ophthalmology, Edward S. Harkness Eye Institute, College of Physicians and Surgeons, Columbia University, 635 West 165th Street, Research Annex Room 715, New York, NY 10032 USA.
e-mail: dcp14@cumc.columbia.edu

Received: April 12, 2020
Accepted: July 6, 2020
Published: August 11, 2020

Keywords: sodium hydroxymethylglycinate; corneal cross-linking; confocal microscopy; biomechanical inflation testing; corneal reservoir; keratoconus

Citation: Zyablitskaya M, Jayyosi C, Takaoka A, Myers KM, Suh LH, Nagasaki T, Trokel SL, Paik DC. Topical corneal cross-linking solution delivered via corneal reservoir in dutch-belted rabbits. Trans Vis Sci Tech. 2020;9(9):20, https://doi.org/10.1167/tvst.9.9.20

Purpose: A topical corneal cross-linking solution that can be used as an adjunct or replacement to standard photochemical cross-linking (UV-riboflavin) methods remain an attractive possibility. Optimal concentration and delivery method for such topical corneal stabilization in the living rabbit eye were developed.

Methods: A series of experiments were carried out using Dutch-belted rabbits (3 months old, weighing 1.0–1.5 kg) and topical cross-linking solutions (sodium hydroxymethylglycinate) (10–250 mM) delivered via corneal reservoir. The application regimen included a one-time 30-minute application (10–40 mM sodium hydroxymethylglycinate) as well as a once per week 5-minute application (250 mM sodium hydroxymethylglycinate) for 7 weeks. Animals were evaluated serially for changes in IOP, pachymetry, epithelial integrity, and endothelial cell counts. Keratocyte changes were identified using intravital laser scanning confocal microscopy. Post mortem efficacy was evaluated by mechanical inflation testing.

Results: Overall, there were very few differences observed in right eye treated versus left eye controls with respect to intraocular pressure, pachymetry, and endothelial cell counts, although 30-minute cross-linking techniques did cause transient increases in thickness resolving within 7 days. Epithelial damage was noted in all of the 30-minute applications and fully resolved within 72 hours. Keratocyte changes were significant, showing a wound healing pattern similar to that after riboflavin UVA photochemical cross-linking in rabbits and humans. Surprisingly, post mortem inflation testing showed that the lower concentration of 20 mM delivered over 30 minutes showed the most profound stiffening/strengthening effect.

Conclusions: Topical cross-linking conditions that are safe and can increase corneal stiffness/strength in the living rabbit eye have been identified.

Translational Relevance: A topical corneal cross-linking solution delivered via corneal reservoir is shown to be both safe and effective at increasing tissue strength in living rabbit eyes and could now be tested in patients suffering from keratoconus and other conditions marked by corneal tissue weakness.

Introduction

Keratoconus (KCN) treatment includes corrective spectacles and contact lenses for mild KCN, as well as penetrating keratoplasty for advanced KCN. Approximately 10% to 20% of patients with KCN require penetrating keratoplasty, but recent use of noninvasive cross-linking treatments to stabilize KCN progression are decreasing the frequency of penetrating keratoplasty.[1–3] A current focus has been directed to further develop collagen cross-linking treatments to prevent the progression of ectasia and, in particular, KCN. Various methods are under evaluation that include photochemical approaches where either modulation in light application methods (i.e., greater fluence/shorter irradiation times, different wavelengths) and/or changes

in photosensitizer methods (i.e., "epi-on" methods using iontophoresis of other permeability enhancers, alternative photosensitizers) are being tested. In addition, topical solutions are also being considered since they would obviate the need for intentional ultraviolet (UV) light exposure with its theoretical health risks as well as the costs that accompany the acquisition of the UV delivery device, its maintenance, and regulations surrounding its use. These topical solutions include the use of various aldehydes,[4] carbohydrates,[5] genipin,[6] and formaldehyde releasers.[7]

Corneal cross-linking increases tissue strength and imparts greater structural integrity by creating additional covalent bonds within collagen fibrils. Riboflavin UVA cross-linking (CXL) is the standard method to treat corneal tissue in this manner. The traditional CXL method involves presaturating the cornea with a photosensitizer, riboflavin-6-phosphate, after intentional epithelial removal. Direct UVA exposure at approximately 365 nm is then applied for 30 minutes.

In this report, cross-linking treatment with sodium hydroxymethylglycinate (SMG) was evaluated in live rabbits. This report is the first of using SMG in live animal corneas; the previous literature regarding this compound has been carried out in ex vivo systems.[7,8] SMG is a compound from a class of compounds known as formaldehyde-releasing agents (FARs). FARs are in widespread use as chemical preservatives in cosmetics and other personal care products, such as shampoos and conditioners. Because these compounds often come in direct contact with the human body, their safety profiles have been evaluated before their use in people. Given the proper conditions, FARs release formaldehyde to variable degrees.[9] Curiously, although formaldehyde is a known carcinogen, the literature supports the fact that FARs are nonmutagenic and noncarcinogenic.[7] SMG, in particular, has found significant commercial use as a chemical preservative owing to its antimicrobial properties,[10] and is in use in a variety of products that include eyedrop formulations for use in dry eye therapy (Blu-Gel A, Sooft, Italy). Thus, this agent is already being used topically in the human cornea, albeit at lower concentrations than we propose. SMG's relatively smaller size and potent cross-linking effects justified its selection as a candidate corneal cross-linking compound for evaluation in live animals as reported herein.

Thus, the present study was undertaken to identify a concentration and delivery method using SMG that could provide measurable tissue strengthening effects while maintaining safety.

Methods

Animal Care and Experimentation

All experimental procedures were approved by the Institutional Animal Care and Use Committee of Columbia University and were in adherence to the ARVO Statement for the Use of Animals in Ophthalmic and Vision Research. Dutch Belted rabbits aged 14 to 18 weeks ($n = 23$) weighing 1.0 to 1.5 kg were obtained from Covance (Princeton, NJ). After a 1-week acclimatization period, a pretreatment baseline evaluation was completed to ensure that no signs of ocular inflammation or gross abnormalities were present. The animals were housed in standard cages in a light-controlled room at a temperature of 23°C ± 2°C. Animals were housed at a relative humidity of 60% ± 10% and a 12-hour light–dark cycle (6 AM to 6 PM). Animals were given food and water ad libitum. Rabbits were examined for up to 4 months after the treatment began.

Topical anesthesia was applied to enhance corneal epithelial permeability using proparacaine HCL 0.5 9 (Akorn, Lake Forest, IL). Intraocular pressure (IOP) and pachymetry measurements were obtained with the animals fully awake with only topical anesthetic, ensuring proper IOP measurements. For the cross-linking treatment procedure, IVLSCM, and before euthanasia, the animals were sedated with an intramuscular injection of ketamine (25–35 mg/kg) and xylazine (2–3 mg/kg). Euthanasia was performed through the marginal ear vein with an overdose of sodium pentobarbital (Euthasol, Virbac, Fort Worth, TX).

Treatment Groups

SMG solutions (Tyger Chemicals Scientific Inc. [Ewing, NJ] or Ashland Inc. [Columbus, OH]) were produced in various dilutions based on the maximum allowed concentration in cosmetics and other personal care products as determined by the European committee on cosmetic standards. These standards report the maximum allowed concentration of SMG as 0.5%, which is 39.06 mM. We rounded this number to 40 mM of SMG (for ease of computation and communication) using this concentration as our "max allowed" concentration for all subsequent dilutions. Thus, our SMG treatment groups were as follows: group 1 = one-quarter max (10 mM; $n = 3$), group 2 = one-half max (20 mM; $n = 6$), group 3 = three-quarters max (30m M; $n = 3$), group 4 = max (40 mM; $n = 3$), and group 5 = approximately

6× max (250 Mm; $n = 8$). Unbuffered solutions were used for groups 1 through 4 and 0.1 M sodium bicarbonate solution (Sigma-Aldrich Corp., St. Louis, MO) was used for group 5 only. The osmolarity for each solution was measured using a vapor pressure osmometer (Wescor Inc., Logan, UT) and was as follows: group 1 = 189 mOsm, group 2 = 215 mOsm, group 3 = 223 mOsm, group 4 = 250 mOsm, and group 5 = 664 mOsm. The pH of the solutions were 9.6 for the buffered solutions (group 5) and 10.9 for the unbuffered solutions (groups 1–4).

To administer the cross-linking solutions, an 8-mm Hessburg-Barron corneal vacuum reservoir (JEDMED, St. Louis, MO) was attached to the rabbit's corneal surface as per the manufacturer's guidelines using the attached syringe suction apparatus. The 250-mM SMG group (group 5) was treated for 5 minutes. This treatment was repeated on a weekly basis for a total of 7 weeks and was the only group in which repeat treatments were carried out. The subsequent groups (groups 1–4) were all treated as a one-time treatment only but for 30 minutes, with solutions exchanges every 5 minutes. For all the groups, the reservoir was filled with 500 µL of SMG cross-linking solution. Immediately after treatment completion, the treated eye was irrigated with balanced salt solution, and the control contralateral eye was treated identically with the carrier solution. After the procedure, a pea-sized amount of erythromycin ophthalmic ointment USP 0.5% was applied to the treated eye daily for 3 days.

IOP and Pachymetry

IOP and central corneal thickness measurements were taken weekly using a contact tonometer (Tonopen Avia VET Reichter Technologies, Depew, NY) and ultrasound pachymeter (Pachmate, DGH Technologies, PA), respectively. An average of five measurements were recorded for IOP. For pachymetry, the Pachmate automatically captures central corneal thickness values in a set of 25. The software then averages the IOP values and calculates error margins.

Epithelial Evaluation

To detect any epithelium defects, fluorescein staining was conducted in both treatment and control eyes in all groups at baseline and after cross-linking treatment. One drop of fluorescein stain was applied and followed by a saline wash to remove excess fluorescein. Blue light from a handheld ophthalmoscope was then used to evaluate epithelial integrity and a photograph taken or pictorial drawing made of the defect. HRT imaging was also used to evaluate epithelial integrity directly.

IVLSCM

IVLSCM was carried out using the HRT III with Rostock Corneal Module (HRT3-RCM). GenTeal (Novartis, Fort Worth, TX) water based gel was applied for lubrication and as a coupling media and the field of view for each image was 400 × 400 µm. IVLSCM stacks were taken at a rate of 30 frames per second with a predetermined thickness of 60 µm. Images were taken at several locations on the cornea, including the central and peripheral corneal sites, both within the 8-mm diameter reservoir treatment area and peripheral to this zone.

IVLSCM: Sub-Basal Nerves (SBN)

SBNs, located just above Bowman's membrane, at the junction between the epithelium and stroma, were analyzed with IVLSCM stacks that contained the basal epithelial layer. Up to three IVLSCM stacks at different radial locations containing the Bowman's layer was obtained for each rabbit eye. SBN were considered present if SBN (or superficial nerve terminals) were detected in any of the available IVLSCM stacks that contained the Bowman's layer. During image processing, the presence of either superficial nerve terminals or SBN were considered as evidence of nontoxicity to the nerves.

IVLSCM: Stroma

Numerous image stacks were taken from several locations, including the 8-mm diameter treatment zone. Assessments and recording of stromal keratocyte patterning changes were made from the stacks that showed the most predominant cellular changes. Images were taken serially over the course of up to 2 months, including a baseline, pretreatment evaluation in all animals. The predominant changes during each evaluation were noted as a function of cross-linking conditions, time from cross-linking, and depth within the stroma. Stromal morphologic categories were identified based on patterns of cell quiescence, cell death, cell activation, and cell repopulation and are described in Figure 3.

IVLSCM: Endothelium

Single endothelial nonoverlapping images (25 manually selected cells per field) were taken for endothelial cell analysis (HRT3-RCM software

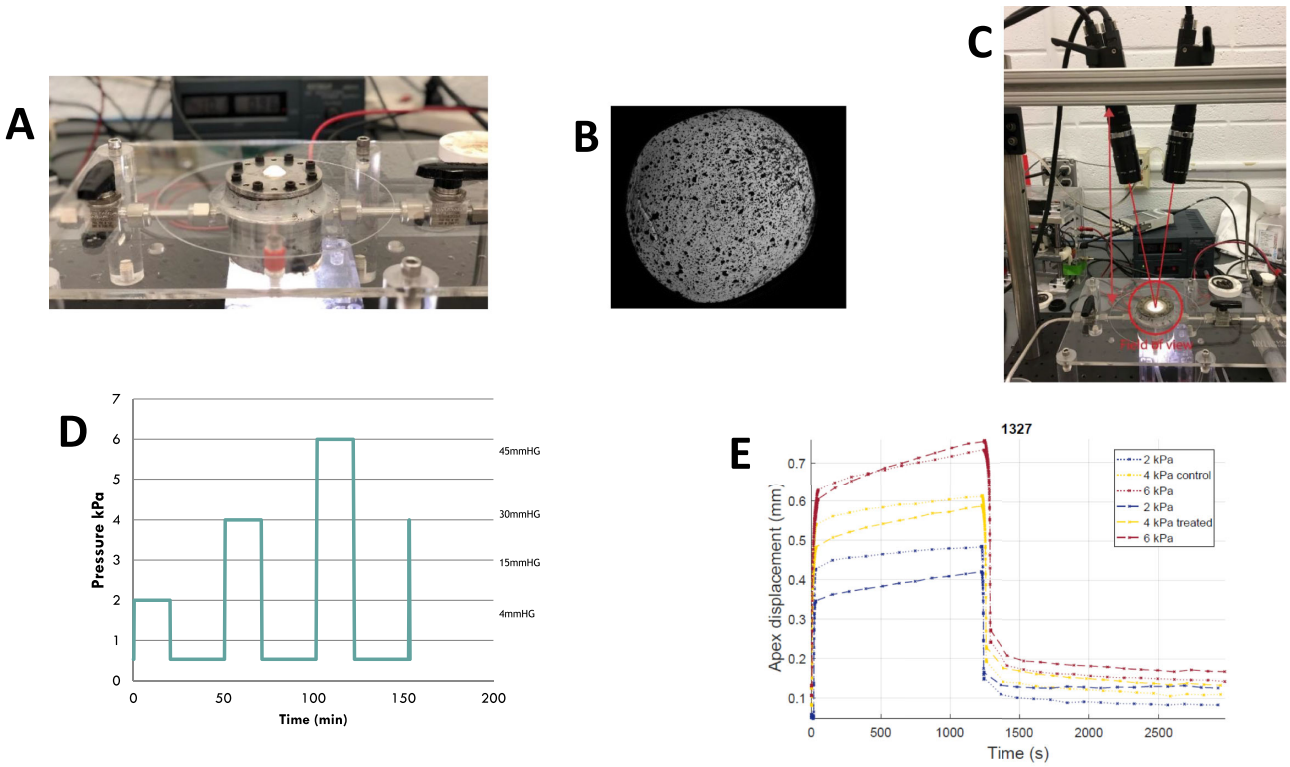

Figure 1. Mechanical inflation testing apparatus and protocol. (A) Picture of mounting plate with corneal sample in place on inflation testing rig. Eight dark-colored locking screws can be seen encircling the corneal sample seen centrally. (B) Enlarged image of corneal sample after graphite ink speckling. (C) Zoomed out view of inflation testing apparatus showing a two-camera system for digital image correlation analysis. (D) Schematic of creep ramp-hold testing protocol. This includes ramp holds at 2, 4, and 6 kPa (15, 30 and 45 mm Hg) with baseline pressure of 0.5 kPa, pressure was held for 20 minutes with pauses of 30 minutes between ramps. (E) Example of data output from ramp-hold testing color-coded for different loads. Control and test samples are denoted by *dotted* (controls) and *dotted-dashed* (cross-linked) *lines*. Apex displacement values for generation of Figure 4 were taken before sample creeping (i.e., at the beginning of the "hold" part of the horizontal part of the curve, after pressurization to 2, 4, or 6 kPa).

Heidelberg Eye Explorer version 1.7.1.0). Total cell density counts were performed in triplicate for each eye and averaged. Cells were counted in a predetermined square box area of the same size for each cornea using the Heidelberg Eye Explorer software. Cells crossing the borders of the boxed selected area were only counted on the left and lower sides of the box to avoid over or under estimations of cell counts and was expressed in cells per square millimeters.

Corneal Inflation Chamber Testing

The method for biomechanical inflation testing with digital image correlation was carried out as previously described by Myers et al.[11,12] and Boyce et al (Figs. 1A–C).[13] After euthanasia of the animal using an intravenous lethal dose injection of sodium pentobarbital (50 mg/kg), the rabbit globes were immediately dissected from the animal and transported to the inflation testing facility on ice wrapped in a saline soaked gauze containing an antiprotease solution (Sigma-Aldrich S8830). The order of sample testing was alternated between treated and nontreated globes to limit the possibility that storage time could impact the results. Pachymetry corneal thickness measurements were taken before dissection and before and after the mechanical tests and were performed using an ultrasound pachymeter.

For the dissection, the cornea with a rim of sclera was isolated from the rest of the eye bulb. The scleral part was glued and clamped between two metal ring holders. The opening hole of the holder on which the pressure was applied and defined our field of view was 1 inch in diameter, which is approximately the diameter of the cornea so that only corneal tissue was subjected to pressurization (Figs. 1A, 1C). Inflation was conducted with saline solution. The inner surface of the cornea was therefore constantly hydrated during the test, while the outer surface was exposed to air but was encased in a humidity chamber. Pressure

control was achieved with a syringe pump controlled with Labview. Before the initiation of testing, corneal surface speckling was performed using an air brush and graphite ink to create a random speckled pattern for digital image correlation (Fig. 1B). Two CCD cameras were positioned above the pressure chamber to image the outer speckled surface of the cornea as it was being pressurized/deformed during loading (Fig. 1C).

Loading Regimen

Loading is adapted from Myers et al.[12] A baseline pressure of 0.5 kPa was applied (Fig. 1D). A series of five loads/unloads between 0.5 and 2.0 kPa with relaxation periods is performed with varying loading rates (0.07, 0.13, and 0.7 kPa/s) to assess the rate dependent properties of the cornea. After this rate-dependent loading regimen, a creep ramp-hold test was performed, loading the cornea to 2, 4, and 6 kPa successively, with the load being held for 20-minute and 30-minute relaxation periods between ramp-holds (Fig. 1D). Loading and unloading during ramp-hold were conducted at 0.13 kPa/s. These ramp-hold evaluations were used primarily for the results reported for these inflations tests as shown in the Results section. Finally, a last load/unload cycle was applied after the last ramp-hold, between 0.5 kPa and 2.0 kPa at 0.13 kPa/s.

Image Analysis and Data Processing

Image acquisition was set to 1 image/sec during loading/unloading periods and 1 image/2 minutes during relaxation periods (Vic-Snap, Correlated Solutions, Inc., Irmo, SC). Optimal lighting was achieved with an LED light underneath the pressurized chamber that projects the shadow of the speckling on the camera sensors (Fig. 1C). A light diffuser was also placed inside the chamber to achieve uniform and less bright lighting conditions.

An image analysis was conducted using Vic 3D (Correlated Solutions, Inc.) to obtain displacement and Green-Lagrange strain fields. The error of the digital image correlation algorithm is estimated following the method described in Myers et al.[12] Briefly, two sets of images taken at baseline pressure are analyzed through Vic3D. The displacement fields obtained (U, V, and W) are used to calculated an error at each correlation point defined as: $E = \mathrm{sqrt}(U^2 + V^2 + W^2)$. An example of the data output, focusing on the apex displacement during ramp-hold loading and unloading is shown in Figure 1E. The apex displacement value was taken from the exact beginning of the "hold" (i.e., horizontal part of the curve in Fig. 1E) after pressurization to 2 kPa (blue), 4 kPa (yellow), or 6 kPa (red).

Results

Epithelium

Epithelial defects (beyond those caused by application of the corneal reservoir) were observed by standard ophthalmologic fluorescein staining and were found to be present in all groups following cross-linking treatment with SMG. In the buffered group 5 (250 mM/5 minutes) the defect was much smaller in size than those noted in the 30-minute unbuffered treatment groups (groups 1–4). The defect typically displayed a jagged irregular shape and occupied the upper third of the cornea within the area of the reservoir application (8 mm in diameter). Curiously, the subsequent six treatments for group 5 did not result in any epithelial defect. In all of the 30-minute treatment groups (1–4), defects were noted and occupied an area of not greater than 6 mm in diameter (i.e., less than corneal reservoir 8-mm diameter). In addition, all the animals showed an 8-mm fluorescent rim defect that corresponded with the suction application from the corneal reservoir. These epithelial defects healed rapidly as evidenced by fluorescein staining, which became negative within 72 hours after treatment. As viewed by confocal microscopy, the epithelial healing process was complete within 7 days after treatment, with full-thickness regeneration with multilayers noted by HRT imaging.

IOP

IOP was measured using the contact tonometer (tonopen) at baseline and throughout the course of the treatment and follow-up periods (Figs. 2A–E). Throughout this time, there were no significant differences observed when comparing treated and control eyes or when comparing values at the beginning of the experiment with the end of the observation period. As shown in Figure 2A through 2E, the solid black (left eye control) and solid grey (right eye treated) lines generally show coherence (or near coherence) starting from the baseline measurements and extending up until 2 months after the cross-linking treatment.

Pachymetry (Corneal Thickness)

In the immediate post–cross-linking period (first 7 days), multiple serial contact evaluations for pachymetry, IOP, and IVLSCM were intentionally avoided in an effort to prevent unnecessary secondary

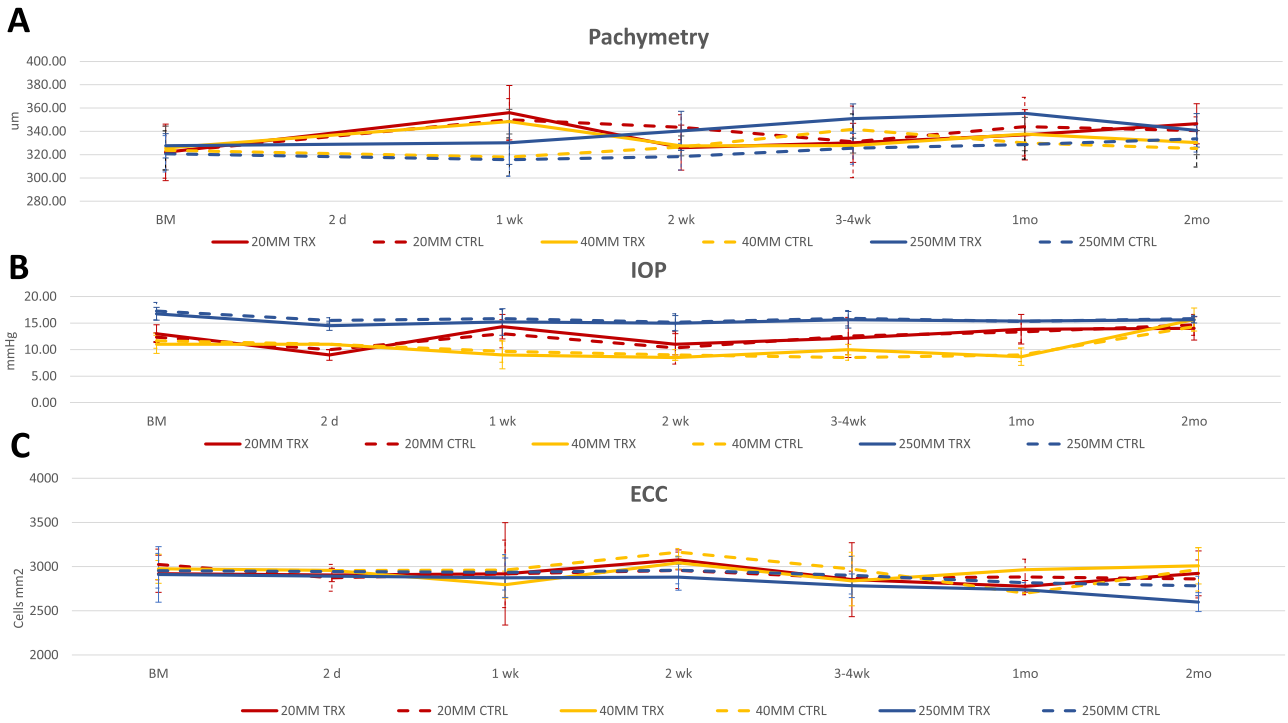

Figure 2. (A) Pachymetry, (B) IOP, and (C) ECC values observed at baseline measurement (BM) and up to 2 months after topical cross-linking with SMG. Results from three different treatment groups are shown and include group 2 (20 mM × 30 minutes; $n = 6$; *red*), group 4 (40 mM × 30 minutes; $n = 3$; *yellow*), and group 5 (250 mM × 5 minutes; $n = 8$; *blue*). Treated groups are shown by *solid lines* and controls groups are shown by *dashed lines*.

mechanical injury to the corneal surface (Figs. 2A–E). Pachymetry measurements for the control and treatment eye are shown in Figure 2A through 2E as orange (right eye treated) and light blue (left eye control) dashed lines, respectively.

Transient corneal thickness increases (data not shown) were noted in all groups and normalized completely by the 7-day evaluation time. For the 250 mM/5-minute group (group 5), corneal thickness increased by 10% following cross-linking as compared with initial thickness and approximately 13% as compared with the control eye measured on the same day. This effect held true for only the first of 7 weekly treatments. The subsequent six treatments did not show similar thickness increases after the identical 250 mM/5-minute procedure. For the 10 mM/30-minute group (group 1), corneal thickness nearly doubled in one animal as compared with the initial pre–cross-linking thickness as well as in comparison with the control eye measured on the same day. For the 20 mM/30-minute group (group 2), corneal thickness increased by about 50% in two animals as compared with initial pre–cross-linking thickness as well as in comparison with the control eye measured on the same day. For the 30 mM/30-minute group (group 3), corneal thickness increased by 28% in one animal after cross-linking as compared with the initial thickness and approximately 27% as compared with the control eye measured on the same day. Finally, for the 40 mM/30-minute group (group 4), corneal thickness increased by 57% of the initial thickness in one animal and was almost 70% thicker as compared with the respective control eye measured on the same day. These initial data points are not shown in Figure 2 because the readings were obtained on only a select few number of animals to prevent secondary trauma to the corneal surface of the treated eyes. All treated corneas returned to their initial thicknesses by 1 week. For both corneas in all rabbits, very little fluctuation in thickness was observed in subsequent measurements during the follow-up period, which was up to 4 months. This included group 5, which had serial cross-linking treatments. Final thicknesses were comparable with initial thicknesses in both treated and control eyes.

IVLSCM Findings

IVLSCM provides a series of high-resolution images, allowing assessment of the depth-dependent changes in cell morphology, density, and reflectivity without the use of microscopic staining methods.

These effects were followed in real-time over the course of up to 3 months.

SBN and Superficial Nerve Terminals

IVLSCM imaging suggest that the SBN plexus seems to have remained unaffected by SMG cross-linking. SBN were consistently present at baseline measurements. Throughout the post-treatment period for all SMG concentrations, SBN were deemed present at each IVLSCM evaluation in both treatment and control eyes. SBN and superficial nerve terminals were often detected simultaneously, but at different locations on the cornea.

Endothelium

Some variability in the ECC were noted for both right and left corneas in all rabbits (Figs. 2A–E), although there was no evidence of a sustained toxic effect from any of the treatment regimens tested. For the majority of ECC evaluations, the largest difference in cell density between the pretreatment and post- treatment corneas was within 200 cells per mm^2. There were, however, a few time points where the difference in ECC between control and treatment eyes increased to as much as 400 cells/mm^2. Of note, the increases in corneal thickness as measured by ultrasound pachymetry at 2 days after treatment did not correlate with ECC decreases although morphologically, the endothelial cells during the first 2 to 3 days seemed to be slightly contracted (see Fig. 3A bottom), but returned to baseline morphology at 1 week after cross-linking.

Stromal Keratocyte Changes

The keratocyte stromal findings were similar between all groups treated with the 30 minute, one-time, method, regardless of concentration (Fig. 3). Keratocyte apoptosis within the first few days after treatment was suggested by the loss of normal-appearing hyper-reflective keratocyte nuclei and occurred within 1 to 3 days after SMG cross-linking treatment. This was shown as either acellular zones (Fig. 3B) that could contain cell debris and haze; or anuclear cell remnants, either hyporeflective (Fig. 3C) or hyper-reflective (Fig. 3D). In many cases, only a few hyper-reflective keratocytes nuclei were observed against the dark background of the extracellular matrix (see Fig. 3).

Morphologic features of keratocyte activation in our study included the identification of hyper-reflective, spindle-like structures, both long (Fig. 3F) and short (Fig. 3G), representing activated migrating keratocytes as well as thick band structures (Fig. 3E) that may represent disorganized hyper-reflective extracellular matrix material in conjunction with spindle-like hyper-reflective cellular structures. These large hyper-reflective bands (i.e., thick bands) have been seen in the post-CXL human cornea and have been described as fibrillar deposits[14] and large hyper-reflective bands.[15] The thick bands generally appeared between week 1 and week 3 and were gradually replaced by long/short spindles and cell clumping by week 4. These spindle-like keratocyte structures are typical stigmata for activated migrating keratocytes after injury. As the healing process continued, the long spindles became less evident with the short spindles and cell clumping structures becoming the dominant findings from the week 4 to week 8 time frame. Stromal cellularity generally recovered to its pre–cross-linking state by 2 to 3 months, with some remnants of cell clumping and occasional spindles.

By comparison with these groups, the animals treated serially over 7 weeks using the 5-minute/high-concentration method showed that the effect on stromal keratocytes were more superficial and less consistent with respect to the timing of changes seen, which is likely due to the fact that the treatments occurred serially (once per week) over 7 weeks. In these animals, either individual spindle-like cells or thicker cell aggregations in the thick band-like form were observed. This group did not show a uniform pattern of changes in the treated area by comparison with the 30-minute treated groups. Depending on the location within the cornea, there were areas with different degrees of cell proliferation and different degrees of keratocyte activation as well as areas of normal appearing keratocytes. In other words, the areas of cell changes were more sporadic than those observed in the 30-minute, one-time treatment groups.

Light Microscopy

There were no histologic abnormalities observed in the eyelid, iris, trabecular meshwork, lens, or retina in the treated tissues, as viewed using standard hematoxylin and eosin staining (images not shown).

Inflation Chamber Testing – Apex Displacement

The average apex displacements are shown in Figure 4. As shown in Figure 4, mechanical inflation testing confirmed increased tissue stiffness in SMG

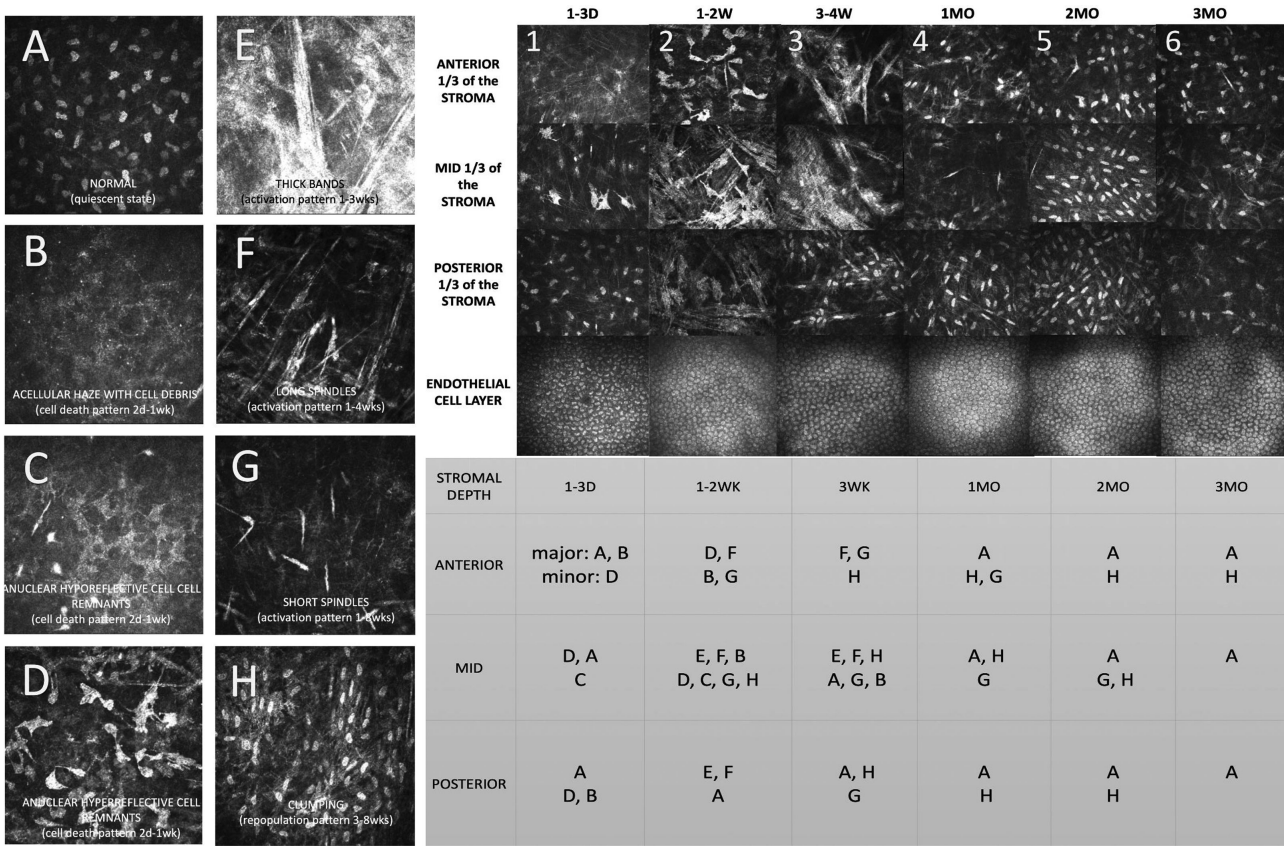

STROMAL DEPTH	1-3D	1-2WK	3WK	1MO	2MO	3MO
ANTERIOR	major: A, B minor: D	D, F B, G	F, G H	A H, G	A H	A H
MID	D, A C	E, F, B D, C, G, H	E, F, H A, G, B	A, H G	A G, H	A
POSTERIOR	A D, B	E, F A	A, H G	A H	A H	A

Figure 3. (*Left side*) Stromal morphologic patterns observed following topical cross-linking with SMG solutions. Eight keratocyte patterns were observed by IVLSCM related to the cross-linking procedure as follows: (A) a normal quiescent keratocyte pattern with or without keratocyte cytoplasmic shadows. Loss of cell nuclei signifying that cell death had occurred or was occurring was seen as three different patterns as follows: (B) acellular with haze, (C) anuclear hyporeflective cell remnants, or (D) anuclear hyper-reflective cell remnants. These three cell death patterns were associated with punctate hyper-reflective cell debris and were seen at 1 to 3 days but could be seen for up to 1 week after the 30-minute procedure. The cell death patterns were followed by (with overlap) signs of keratocyte activation that included the formation of (E) thick bands owing to both activated keratocyte cytoplasm hyper-reflectivity as well as disorganized extracellular matrix hyper-reflectivity, seen from 1 to 3 weeks; (F) long spindles defined as cytoplasmic hyper-reflective extensions longer than the length of the 3× nuclei, seen from 1 to 4 weeks; and (G) short spindles defined as cytoplasmic hyper-reflective extensions less than the length of 3× nuclei, seen from 1 to 8 weeks. Later in the recovery process, (H) hypercellularity with cell clumping (or aggregation), signifying keratocyte repopulation of the stroma is seen from 4 to 8 weeks. A summary of major and minor morphologic findings for groups 1 to 4 is included as a table at the bottom right. (*Upper right*) Example of time-lapsed representative IVLSCM images following a one-time application of SMG cross-linking treatment of 20 mM (0.25%) for 30 minutes via corneal reservoir. Top *x*-axis from left to right indicates progression of time since baseline measurement (not shown) to time after treatment: 1 to 3 days (column 1), 1 to 2 weeks (column 2), 3 to 4 weeks (column 3), 1 month (column 4), 2 months (column 5), and 3 months (column 6). Left *y*-axis from top to bottom indicates progression from anterior stroma (0–100 µm) to mid stroma (100–200 µm) to posterior stroma (200 to 300 µm) to endothelium (>300 µm). In column 1 (1–3 days), acellularity and anuclear cell remnants and debris are observed in the anterior and mid stroma signifying cell death processes. Some cell contraction is seen in the endothelial layer. In column 2 (1–2 weeks), hyper-reflective anuclear cell remnants are seen anteriorly with thick bands forming in the mid and posterior stroma as well as long and short spindles. In column 3 (3 weeks), thick bands are again seen in the anterior and mid stroma with some cell clumping noted posteriorly. Later, in column 4 (1 month) areas of cell clumping and short spindles are seen in the anterior and mid stroma. Hypercellularity with cell clumping is observed in columns 5 (2 months) and baseline quiescent morphology is seen in column 6 (3 months).

cross-linked samples in pressure ranges mimicking physiologic IOP (15–45 mm Hg = 2–6 kP).

The results of a more detailed analysis of strain fields will be reported elsewhere. Here, we present apex displacement data from the study as a simple yet reasonable method of determining whether the cornea was stiffened by the treatment. As should be expected based on the loading protocol used, increasing loads resulted in greater displacements in all samples tested. However, the differences between treated and controls was most striking for group 2 (20 mM SMG × 30 minutes × 1) with delta

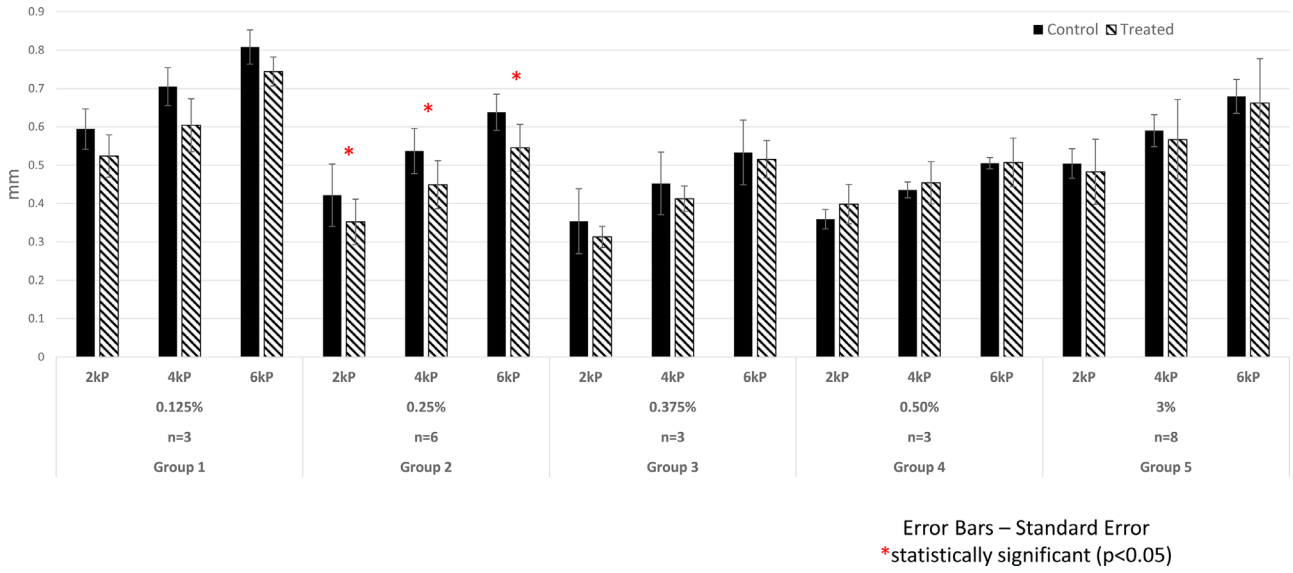

Figure 4. Mechanical inflation testing results. Apex displacement. Post mortem mechanical testing of corneas was carried out as described in Myers et al.[11,12] and Boyce et al.[13] The results of mechanical inflation ramp-hold tests are shown in bar graph form. Apex displacement values are shown for all five groups with results for both left (*control blue*) and right (*treated orange*) eyes shown side by side. Results for three different loads are shown at 2 kP (15 mm Hg), 4 kP (30 mm Hg), and 6 kp (45 mm Hg). The stiffening effect is indicated by differences in apex displacement between left and right eyes with a lesser amount of apex displacement indicating a stiffer cornea. Statistical significance at a *P* value of less than 0.05 was noted for the 20-mM group 2 (0.25%) (shown with an asterisk). A trend in the expected direction was noted for all the remaining groups with the exception of groups 4 and 5, which did not show a consistent stiffening effect.

average apex displacements (control-treated displacements) of 0.0827, 0.0969, and0.0855 at 2, 4, and 6 KPa, respectively. This was the only group in which statistical significance was achieved at a P value of less than 0.05 between treated and untreated control paired corneal samples. Average delta apex displacements for group 1 (10 mM) and group 3 (30 mM) treated samples did not show statistical significance (at $P < 0.05$), although a trend in the expected direction was observed. Group 4 (40 mM), the highest concentration group for 30-minute cross-linking and group 5 (250 mM $\times$ 5 minutes), did not show an expected trend in stiffness, with roughly equivalent apex displacements noted in both treated and control samples. Thus, the use of lower concentrations of SMG in the cross-linking solutions showed increased mechanical stiffening effects by comparison to higher SMG concentrations.

Discussion

The corneal wound healing response is complex and can vary based on the nature and degree of injury. Components of the response include keratocyte death (apoptosis and necrosis), followed by migration of activated fibroblasts into the wounded area to effect repair (as well as myofibroblast transformation in some cases), and concluding with the repopulation of quiescent keratocytes. After the initial injury, the wound response is hall-marked by keratocyte apoptosis, activation, proliferation, migration, and increased extracellular matrix reflectivity. Keratocyte activation can be seen morphologically in the post-injury cornea with the appearance of "spindle-like" cells. Being compared with a fibroblast, the first spindle-like cell appearance was described in corneas after photorefractive keratectomy or keratotomy.[16] Readjusted levels of intracellular keratocyte corneal crystallins (aldehyde dehydrogenase 1 and transketolase), which play a role in the transparency of the cornea, could be responsible for this change in light transmission in the keratocyte.[17]

In our study, initial keratocyte apoptosis cellular changes were followed by (observed at different depths) hyper-reflective spindle-like structures with long or short processes. These spindle-like cells (long and short) (Figs. 3F, 3G) and thick band structures (Fig. 3E) observed in this study were most likely migrating activated keratocytes based on a similar morphology to those described in the corneal wound healing process.[18] Furthermore, such areas of increased cell migration and activation were similar to HRT findings reported in rabbits and patients following CXL.[19] Notably, hyper-reflective band-like structures in our

study were still present 2 to 4 weeks after treatment. Changes in the anterior, mid, and posterior stroma were seen at 1 week after treatment and normalized by week 8 using this method in contrast to CXL literature that suggests a much longer time frame for repopulation to occur[15,20] (i.e., 4–6 months in humans). Thus, the return to normalization may be faster using our method.

There are different factors that could contribute to the degree of keratocyte apoptosis, activation, and repopulation. This has been shown in studies using different methods of photochemical cross-linking (or CXL) as well as an accumulated body of evidence compiled from studies on wound healing after laser ablation (photorefractive keratectomy and LASIK), and cryoinjury. The CXL technique and its various modified forms that include epi-on (or transepithelial) riboflavin cross-linking with or without iontophoretic augmentation; accelerated (using shorter exposure times with increased, pulsed light energy); and in combination with refractive surgery have been studied using in vivo confocal microscopy. The ultimate keratocyte population density can remain stable or change and may present a variable rate of cell death or toxicity response depending on the CXL method, for example, transepithelial versus "epi-off"[20] with accelerated versus conventional methods. In addition, UV light irradiance, epithelial integrity, and method of epithelial debridement may all play contributing roles to keratocyte apoptosis and the toxicity response after cross-linking treatment.

Counterintuitively, the increased stiffening effects were found to be greater and more consistent in the 20-mM group 2 than in the higher concentration 40-mM group 4, which showed equivocal inflation findings by comparison. This effect trend was unexpected, because prior studies using ex vivo eyes have shown that the cross-linking effect increases with increasing concentration in this same concentration range, and thus, the 40-mM samples were expected to have greater stiffness effects, not less, as we observed. The reasons for this paradoxical effect are unclear; however, one reason could be related to differences in the method of cross-linking analysis used in the two studies, which was thermal denaturation for the in vitro study[7] and inflation testing in this live animal treatment study. This difference in concentration-dependent effects could also be a reflection of cross-linking performed in living eyes as opposed to post mortem eyes. In particular, corneal hydration and transcorneal fluid migration could differ significantly between live and dead samples and account for this inconsistency. Finally and importantly, there are differences attributed to wound healing effects that become apparent in live animal studies that could not be accounted for by ex vivo studies that are time limited.

It is likely, however, that the chemical mechanisms that induce the covalent bonds in the extracellular matrix (i.e., fixation) are also responsible for the killing of cells (i.e., toxicity). In this respect, it remains unclear as to the role that the corneal wound healing process plays in the timing of subjective visual changes following CXL. In other words, how important to the clinical effects is the repopulation of keratocytes after CXL? Stated in a different way, is it necessary to kill keratocytes to induce cross-linking stabilizing effects? Furthermore, is there an optimal balance that can be identified, where toxicity is limited and yet efficacy (fixation) is adequate? We believe that these are relevant questions that could impact and should inform the way that we use therapeutic cross-linking methods for not only the cornea but potentially other tissues.

Given the physiologic role of the corneal innervations, preservation of the SBN is crucial and our method was found to preserve the sub-basal corneal nerves. Corneal nerves regulate corneal sensitivity, reflex arch integrity, epithelial proliferation, and wound healing.[21] Patients with KCN may already exhibit abnormal SBN architecture, and SBN density is found to be significantly lower in KCN patient corneas.[21–23] Traditional cross-linking procedures cause significant SBN loss resulting in a relatively anesthetic cornea initially.[20] The mean corneal SBN were significantly lower at 6 months in patients who underwent either conventional or accelerated cross-linking, both of which involved epithelium removal.[24] That being said, the corneal SBN plexus is a dynamic structure and reinnervation to preoperative values have been reported to occur by 12 months after standard CXL cross-linking.[15] Patients with KCN may already have an impaired tearing reflex and corneal sensitivity.[25] Therefore, loss of SBN from cross-linking may prevent maximum treatment benefits and lengthen the recovery period. In our experiment, SMG cross-linking displayed minimal changes to SBN, which can facilitate recovery and maximize treatment outcomes, a potential advantage of our approach over current photochemical therapy.

Fluctuation in the IOP was noted and may have been due to inconsistent hours of measurements during the day. In other words, IOP measurements were taken at various times of the day. Normal IOP for rabbits is within 12 to 17 mm Hg and depends on the time of day.[26] Change in IOP can correlate with the stiffness of the cornea.[27] Even though such an effect might be expected, it was not found to be significantly different in the treated eye and in particular in the eyes that showed an increased stiffness by inflation testing.

Swelling of the cornea within the first few days after the treatment might be explained in part by the disrupted epithelial integrity revealed by the increased uptake of a fluorescein dye (Figs. 1A–D), because endothelial cell counts did not change significantly. That being said, some subtle morphologic endothelial cell changes could be observed early after the cross-linking sessions (some cell contraction) and could have been accompanied by functional alterations in water pumping function. In any event, the swelling was transient and baseline levels were noted following the SMG application within 7 days. Of note, significant swelling with endothelial cell loss has been reported after CXL in rabbits.[28] Of note in our study, the increased thickness effects were greater in the unbuffered solutions groups (1–4) with higher pH although the time of exposure was also longer (30-minute vs. 5 minutes), albeit with lower concentrations (10–40 mM vs. 250 mM).

In conclusion, we have presented live animal corneal cross-linking results using a topical solution approach and have shown that the method is both safe and effective for corneal strengthening. Further translational studies and product development should now occur.

Acknowledgments

The authors thank Jimmy Duong from the Design and Biostatistics Resource and the Biostatistical core facility of the Irving Institute at Columbia University Medical Center for biostatistical consultation.

Patents issued through Columbia University: U.S. Patent Nos. 8,466,203; 9,125,856; 10,105,350; and 10,292,967.

Supported by Research to Prevent Blindness and by National Institutes of Health Grants NEI R01EY020495 (dcp), NEI P30 EY019007, and NCRR UL1RR024156.

Disclosure: **M. Zyablitskaya,** None; **C. Jayyosi,** None; **A. Takaoka,** None; **K.M. Myers,** None; **L.H. Suh,** None; **T. Nagasaki,** None; **S.L. Trokel,** None; **D.C. Paik,** None

References

1. Romero-Jimenez M, Santodomingo-Rubido J, Wolffsohn JS. Keratoconus: a review. *Cont Lens Anterior Eye*. 2010;33:157–166; quiz 205.
2. Mas Tur V, MacGregor C, Jayaswal R, O'Brart D, Maycock N. A review of keratoconus: diagnosis, pathophysiology, and genetics. *Surv Ophthalmol*. 2017;62:770–783.
3. Kennedy RH, Bourne WM, Dyer JA. A 48-year clinical and epidemiologic study of keratoconus. *Am J Ophthalmol*. 1986;101:267–273.
4. Spoerl E, Huhle M, Seiler T. Induction of cross-links in corneal tissue. *Exp Eye Res*. 1998;66:97–103.
5. Spoerl E, Seiler T. Techniques for stiffening the cornea. *J Refract Surg*. 1999;15:711–713.
6. Avila MY, Gerena VA, Navia JL. Corneal crosslinking with genipin, comparison with UV-riboflavin in ex-vivo model. *Mol Vis*. 2012;18:1068–1073.
7. Babar N, Kim M, Cao K, et al. Cosmetic preservatives as therapeutic corneal and scleral tissue cross-linking agents. *Invest Ophthalmol Vis Sci*. 2015;56:1274–1282.
8. Zyablitskaya M, Takaoka A, Munteanu EL, Nagasaki T, Trokel SL, Paik DC. Evaluation of therapeutic tissue crosslinking (TXL) for myopia using second harmonic generation signal microscopy in rabbit sclera. *Invest Ophthalmol Vis Sci*. 2017;58:21–29.
9. Takaoka A, Cao K, Oste EM, Nagasaki T, Paik DC. Topical therapeutic corneal and scleral tissue cross-linking solutions: in vitro formaldehyde release studies using cosmetic preservatives. *Biosci Rep*. 2019;39:BSR20182392.
10. Amponin DE, Przybek-Skrzypecka J, Zyablitskaya M, et al. Ex vivo anti-microbial efficacy of various formaldehyde releasers against antibiotic resistant and antibiotic sensitive microorganisms involved in infectious keratitis. *BMC Ophthalmol*. 2020;20:28.
11. Myers KM, Cone FE, Quigley HA, Gelman S, Pease ME, Nguyen TD. The in vitro inflation response of mouse sclera. *Exp Eye Res*. 2010;91:866–875.
12. Myers KM, Coudrillier B, Boyce BL, Nguyen TD. The inflation response of the posterior bovine sclera. *Acta Biomater*. 2010;6:4327–4335.
13. Boyce BL, Grazier JM, Jones RE, Nguyen TD. Full-field deformation of bovine cornea under constrained inflation conditions. *Biomaterials*. 2008;29:3896–3904.
14. Croxatto JO, Tytiun AE, Argento CJ. Sequential in vivo confocal microscopy study of corneal wound healing after cross-linking in patients with keratoconus. *J Refract Surg*. 2010;26:638–645.
15. Jordan C, Patel DV, Abeysekera N, McGhee CN. In vivo confocal microscopy analyses of corneal

microstructural changes in a prospective study of collagen cross-linking in keratoconus. *Ophthalmology*. 2014;121:469–474.
16. Weimar V. The transformation of corneal stromal cells to fibroblasts in corneal wound healing. *Am J Ophthalmol*. 1957;44:173–180; discussion 180-172.
17. Jester JV, Moller-Pedersen T, Huang J, et al. The cellular basis of corneal transparency: evidence for 'corneal crystallins'. *J Cell Sci*. 1999;112:613–622.
18. Petroll WM, Kivanany PB, Hagenasr D, Graham EK. Corneal fibroblast migration patterns during intrastromal wound healing correlate with ECM structure and alignment. *Invest Ophthalmol Vis Sci*. 2015;56:7352–7361.
19. Hovakimyan M, Falke K, Stahnke T, et al. Morphological analysis of quiescent and activated keratocytes: a review of ex vivo and in vivo findings. *Curr Eye Res*. 2014;39:1129–1144.
20. Mazzotta C, Hafezi F, Kymionis G, et al. In vivo confocal microscopy after corneal collagen crosslinking. *Ocul Surf*. 2015;13:298–314.
21. Cruzat A, Pavan-Langston D, Hamrah P. In vivo confocal microscopy of corneal nerves: analysis and clinical correlation. *Semin Ophthalmol*. 2010;25:171–177.
22. Patel DV, McGhee CN. Mapping the corneal subbasal nerve plexus in keratoconus by in vivo laser scanning confocal microscopy. *Invest Ophthalmol Vis Sci*. 2006;47:1348–1351.
23. Niederer RL, Perumal D, Sherwin T, McGhee CN. Laser scanning in vivo confocal microscopy reveals reduced innervation and reduction in cell density in all layers of the keratoconic cornea. *Invest Ophthalmol Vis Sci*. 2008;49:2964–2970.
24. Bouheraoua N, Jouve L, El Sanharawi M, et al. Optical coherence tomography and confocal microscopy following three different protocols of corneal collagen-crosslinking in keratoconus. *Invest Ophthalmol Vis Sci*. 2014;55:7601–7609.
25. Dogru M, Karakaya H, Ozcetin H, et al. Tear function and ocular surface changes in keratoconus. *Ophthalmology*. 2003;110:1110–1118.
26. Pereira FQ, Bercht BS, Soares MG, da Mota MG, Pigatto JA. Comparison of a rebound and an applanation tonometer for measuring intraocular pressure in normal rabbits. *Vet Ophthalmol*. 2011;14:321–326.
27. Liu J, He X. Corneal stiffness affects IOP elevation during rapid volume change in the eye. *Invest Ophthalmol Vis Sci*. 2009;50:2224–2229.
28. Hovakimyan M, Guthoff R, Knappe S, et al. Short-term corneal response to cross-linking in rabbit eyes assessed by in vivo confocal laser scanning microscopy and histology. *Cornea*. 2011;30:196–203.